Author Manuscript

Author Manuscript

Author Manuscript

Author Manuscript

HHS Public Access

Author manuscript

Sci Immunol. Author manuscript; available in PMC 2021 September 19.

Published in final edited form as:

Sci Immunol. 2021 March 19; 6(57): . doi:10.1126/sciimmunol.abd8003.

Exploiting albumin as a mucosal vaccine chaperone for robust generation of lung-resident memory T cells

Kavya Rakhra[1,2], **Wuhbet Abraham**[1,2], **Chensu Wang**[1,2], **Kelly D. Moynihan**[1,3], **Na Li**[1,2], **Nathan Donahue**[1], **Alexis D. Baldeon**[1], **Darrell J. Irvine**[1,2,3,4,*]

[1]Koch Institute for Integrative Cancer Research, Massachusetts Institute of Technology, Cambridge, MA 02139 USA

[2]Ragon Institute of Massachusetts General Hospital, Massachusetts Institute of Technology and Harvard University, Cambridge, MA 02139 USA

[3]Department of Biological Engineering, Massachusetts Institute of Technology, Cambridge, MA 02139 USA

[4]Howard Hughes Medical Institute, Chevy Chase, MD 20815 USA

Abstract

Tissue-resident memory T cells (T_{RMs}) can profoundly enhance mucosal immunity, but parameters governing T_{RM} induction by vaccination remain poorly understood. Here we describe an approach exploiting natural albumin transport across the airway epithelium to enhance mucosal T_{RM} generation by vaccination. Pulmonary immunization with albumin-binding amphiphile-conjugates of peptide antigens and CpG adjuvant (amph-vaccines) increased vaccine accumulation in the lung and mediastinal lymph nodes (MLNs). Amph-vaccines prolonged antigen presentation in MLNs over 2 weeks, leading to 25-fold increased lung-resident T-cell responses over traditional immunization and enhanced protection from viral or tumor challenge. Mimicking such prolonged exposure through repeated administration of soluble vaccine revealed that persistence of both antigen and adjuvant was critical for optimal T_{RM} induction, mediated through T-cell priming in MLNs post prime, and directly in the lung tissue post boost. Thus, vaccine persistence strongly promotes T_{RM} induction, and amph-conjugates may provide a practical approach to achieve such kinetics in mucosal vaccines.

One-sentence summary:

Pulmonary immunization with albumin-binding peptide vaccines promotes resident memory $CD8^+$ T cell generation in the lung.

*Correspondence to: djirvine@mit.edu.

Author Contributions: KR designed, performed in vivo experiments, analyzed and interpreted data and wrote the manuscript, KDM synthesized amph-CpG and amph-Trp1, Trp2 and gp100, CW performed and analyzed experiments, WA, NL, ND, and AB provided technical support for in vivo studies, DJI conceptualized the experiments, interpreted the data and wrote the manuscript.

Competing interests: DJI and KDM are inventors on a patent application based on use of amphiphile vaccine technology. The patent has been licensed to Elicio Therapeutics, a company co-founded by DJI. The other authors declare that they have no competing interests.

Data and Materials Availability: All additional data needed to evaluate the conclusions in the paper are present in the paper or the Supplementary Materials.

Author Manuscript Author Manuscript Author Manuscript Author Manuscript

Introduction

Tissue-resident memory T cells (T_{RMs}) provide immune surveillance at barrier tissues and provide a first line of defense against intracellular pathogens at mucosal surfaces (1–3). T_{RMs} provide rapid protection in the tissue by detecting antigens presented by infected cells, triggering production of inflammatory cytokines/chemokines and mediating cytotoxicity (1, 4, 5). Studies profiling T_{RM} specificity in different tissues have shown that the human T_{RM} repertoire, while diverse, can be biased towards pathogens that infect a particular tissue, as evidenced by the presence of influenza-specific T_{RMs} in lungs (6, 7) and hepatitis B-specific T_{RMs} in the liver (8). In addition, T_{RMs} play an important role in protection from tumors that develop from epithelial tissues (9–11). Based on these characteristics, the design of vaccines that efficiently generate T_{RM} cells is of great interest for both infectious disease and cancer. Although much progress has been made in defining cues that promote T_{RM} generation (12–15), it remains poorly understood how parameters of vaccination might be optimized to enhance the differentiation of long-lived tissue-resident lymphocyte populations.

Peptide-based vaccines are attractive for their safety, affordability, and compatibility with rapid manufacture for personalized cancer vaccines (16). While numerous ongoing clinical trials are exploring the use of peptide vaccines in cancer (17, 18) and infectious diseases (16, 19), their immunogenicity remains modest and there are currently no FDA-approved peptide vaccines. One major shortcoming of peptide-based vaccines is poor pharmacokinetics, a combination of inefficient accumulation in lymph nodes and rapid degradation *in vivo* (20, 21). To address this, we previously described a vaccine technology enabling massive expansion of antigen-specific T cells, based on coupling peptide antigens or molecular adjuvants to an amphiphilic phospholipid moiety, forming amphiphile vaccines (amph-vaccines) (20–22). On injection, the lipid tail of these amph-vaccine molecules binds to endogenous albumin in the interstitial fluid, and albumin then serves as an efficient chaperone delivering the antigen or adjuvant to draining lymph nodes. In lymph nodes, the lipid tail of the amph-vaccine transfers from albumin to insert in cell membranes, resulting in potent antigen-specific effector $CD8^+$ T-cell responses (21, 22).

Albumin is the most abundant serum protein and like IgG, binds to the neonatal Fc receptor (FcRn), which delays its catabolism and increases its half-life (23). FcRn receptors expressed by pulmonary epithelial cells in the lungs, bi-directionally transport albumin and antibodies across the airway epithelium (23, 24). We hypothesized that amph-vaccines administered to the pulmonary mucosa could be transported from the airway to the lung parenchyma by albumin, and thereafter trafficked to lung-draining lymph nodes to prime tissue-resident T cells.

Here we show that vaccines comprised of peptide antigens and the Toll-like receptor-9 (TLR-9) agonist CpG DNA as a molecular adjuvant, show greatly enhanced uptake in lung tissue when administered as albumin-binding amphiphile conjugates, leading to potent T-cell priming in lung-draining MLNs. Pulmonary immunization with amph-vaccines elicited a long-lived T_{RM} population in the lungs that protected against viral challenge and tumor lung metastasis. Mechanistically, amph-vaccines elicited sustained antigen presentation in MLNs. Mimicking sustained vaccine exposure by repeated administration of unmodified

Author Manuscript Author Manuscript Author Manuscript Author Manuscript

peptide/CpG revealed that optimal establishment of T_{RMs} required prolonged availability of both antigen and adjuvant over ~2 weeks in MLNs and local lung tissue. This leads to efficient T-cell priming in MLNs during a primary immunization and expansion of cells locally in the lung following boosting. These findings provide insights into vaccine characteristics that can be optimized to amplify T_{RM} induction for mucosal immunity.

Results

Albumin-binding vaccines accumulate in the lung parenchyma and draining MLNs

In agreement with previous reports (25), we measured ~200 μg/mL of albumin present in the bronchoalveolar lavage (BAL) fluid of naive mice, which rapidly increased to a few mg/mL following pulmonary administration of the TLR9 agonist CpG (Fig. 1A). Fluorescently-labeled albumin administered intratracheally (i.t.) was retained in the tissue after 24 hr at higher levels in wild type mice than *FcRn*$^{-/-}$ mice, suggesting uptake in the tissue is promoted by FcRn receptors (Fig. 1B–C).

To test whether an albumin-binding moiety would alter tissue distribution of peptide antigens or adjuvants in the lungs, we synthesized amphiphile-conjugate (amph-conjugate) vaccines comprised of a melanoma peptide antigen $gp100_{20–39}$ linked to a DSPE phospholipid tail through a poly(ethylene glycol) spacer, and CpG DNA linked to a similar C18 lipid tail (fig. S1). We previously demonstrated that these amph-conjugate molecules bind to albumin and efficiently traffic to skin-draining lymph nodes following subcutaneous (s.c.) injection (20, 21). We first compared the tissue distribution of fluorescently-labeled free or amph-conjugate $gp100_{20–39}$ and CpG following pulmonary administration in the lungs and lung-draining MLNs, using i.t. instillation as a surrogate for aerosol delivery in humans.

Twenty-four hours after i.t. administration, amph-gp100 conjugates were present in the tissue parenchyma at ~10-fold greater levels than the free peptide, and were still readily detectable 48 hours post immunization (Fig. 1D–E). Amph-gp100 further accumulated in MLNs, with significantly higher levels detected at 48 hours compared to soluble gp100 (Fig. 1D, F). Similarly, amph-CpG showed substantially greater accumulation in the lung tissue and MLNs compared to free CpG (Fig. 1G–I). Together, these results suggest that modification with an albumin-binding lipid tail enhanced the uptake and persistence of peptide antigens and CpG adjuvant in lung tissues.

Pulmonary vaccination with amph-vaccines elicits high levels of antigen-specific lung T_{RMs}

We next evaluated the immunogenicity of amph-vaccines and their ability to prime lung parenchyma-homing T cells compared to the same vaccines administered parenterally. We tested both the gp100 antigen and a viral gag peptide termed AL11 (26), in anticipation of testing for protection against viral challenge. Groups of mice were vaccinated i.t. or s.c. on days 0 and 14 with either free AL11/CpG or amph-AL11/amph-CpG. One week later, tissues were collected and intravascular staining was used to differentiate T cells localized in the vasculature vs. the lung parenchyma (27). In accordance with our previous results (20),

Author Manuscript Author Manuscript Author Manuscript Author Manuscript

amph-conjugate vaccination elicited much greater AL11-specific T-cell expansion in the peripheral blood compared to soluble peptide/CpG immunization whether administered s.c. or i.t., but s.c. amph-vaccination elicited higher levels of circulating T cells than i.t. administration (Fig. 2A, B). By contrast, i.t. amph-vaccines elicited a large population of antigen-specific T cells in the lungs, 25-fold greater than soluble peptide/CpG given by the same route and 100-fold greater than amph-vaccines administered subcutaneously (Fig. 2A, C). We carried out similar experiments with soluble vs. amph-conjugate gp100/CpG vaccines, and evaluated the functionality of the resulting T-cell responses 1-week post boost via intracellular cytokine staining. As shown in fig. S2A–C, s.c.-delivered amph-vaccination elicited a strong IFN-γ/TNF-α-producing gp100-specific T-cell response in the lung vasculature, but essentially no cytokine-competent T cells were detected in the lung parenchyma. By contrast, pulmonary vaccination elicited a prominent population of cytokine-producing T cells in the lung tissue, with amph-conjugate immunization eliciting a 24-fold larger cytokine$^+$ T-cell response compared to soluble vaccines (fig. S2C).

CD8$^+$ T cells in the lung parenchyma following amph-conjugate vaccination expressed substantially higher levels of the collagen-binding mucosal $\alpha_1\beta_1$ integrin CD49a compared to cells in the peripheral blood or lung vasculature (Fig. 2D) (28). The majority of lung antigen-specific CD8$^+$ T cells following i.t. immunization also expressed the tissue-resident markers CD69, CD103, or both, while T cells primed by the parenteral immunizations expressed these markers at a much lower frequency (Fig. 2E–F) (29–31).

Similar to our previous findings with parenteral amph-peptide vaccination (21), T-cell priming by i.t. amph-vaccine immunization was mediated by Batf3-dependent dendritic cells (DCs), as indicated by the loss of responses in *Batf3*$^{-/-}$ animals (Fig. 2G). Additionally, antigen-specific T-cell responses trended lower in the lungs of *FcRn*$^{-/-}$ mice (Fig. 2H) and the generation of CD69$^+$CD103$^+$ cells was significantly reduced (fig. S3).

Since intranasal (i.n.) immunization is more easily implemented clinically than aerosol immunization, we also compared i.n. and i.t. vaccine delivery. We found that i.t. immunization elicited 4-fold higher T-cell responses in the lungs compared to i.n. immunization (fig. S4). Based on these data, we focused on i.t. administration to mimic aerosol immunization in humans. Collectively, these data suggest that i.t-delivered amph-conjugates greatly enhance the potency of lung mucosal peptide vaccination and that pulmonary amph-vaccines promote establishment of T $_{RM}$s in the lung parenchyma.

Pulmonary vaccination with amph-conjugate vaccines is protective against viral and tumor challenge

To evaluate the persistence of lung T_{RM}s, we primed and boosted mice with soluble or amphiphile-conjugate AL11 gag peptide vaccines, and analyzed lung tissues 4 months post boost (Fig. 3A). A significant population of antigen-specific lung T cells was only detectable in mice that received i.t. amph-vaccination (Fig. 3B–C), and ~25% of these T cells were CD103$^+$ (Fig. 3D). To test the protective capacity of this T_{RM} population, we challenged AL11-vaccinated mice i.t. with a lethal dose of vaccinia virus expressing the gag epitope five months after immunization. Animals that received the amph-vaccine delivered i.t. all survived viral challenge, while mice in all other groups continuously lost body weight and

Author Manuscript Author Manuscript Author Manuscript Author Manuscript

succumbed by day 7 (Fig. 3E, F). To determine whether protection was mediated by cells pre-positioned in the lungs versus recruited from the blood, we repeated this experiment but treated animals with FTY720 starting 5 days before challenge to block egress of T cells from lymph nodes (32) (fig. S5A–B). Protection from viral challenge in mice receiving the i.t. amph-vaccine was not significantly different in cohorts that received FTY720 or the vehicle alone control (Fig. 3G; $p > 0.999$), suggesting that *de novo* T-cell recruitment into the lung was not necessary for protection. Only i.t amph-vaccination significantly reduced viral burden in the lungs compared to non-vaccinated mice (Fig. 3H). FTY720 treated i.t.-vaccinated mice showed a trend toward higher viral loads in the lungs but this did not reach statistical significance, suggesting that protection was predominantly mediated by T_{RMs}.

To test the protective capacity of mucosal amph-conjugate vaccination against tumors, we prophylactically vaccinated mice with amph-conjugates of three melanoma peptides ($Trp1_{455–463}$, $Trp2_{180–188}$ and $gp100_{20–39}$) and challenged animals 30 days later with an intravenous injection of B16F10 melanoma cells. A majority of animals were protected in the pulmonary-vaccinated group while only 40% were protected by s.c. vaccination, although these data did not reach statistical significance (Fig. 3I). To evaluate the potential of amph-vaccines to be useful in a therapeutic context, we performed a study treating B16F10 lung metastases with amph-vaccination in the presence of clinically-relevant checkpoint blockade. While anti-PD1 alone had no efficacy in this setting, 60% of mice treated with amph –vaccine + anti-PD1 showed complete tumor regression (fig. S6). Thus, amph-conjugate vaccination primed a long-lived pool of antigen-specific T cells in the lungs that was protective against viral or tumor challenge.

Sustained exposure to antigen and adjuvant in MLNs enhances T_{RM} generation in lungs

We next sought to understand why amph-conjugate vaccination was so much more effective in generating T_{RM} cells compared to soluble peptide immunization. We hypothesized that the duration of antigen presentation elicited by amph-conjugate vaccines might be an important factor contributing to the formation of T_{RMs}. To define the kinetics of antigen presentation resulting from soluble vs. amph-conjugate vaccination, we immunized mice i.t. with either soluble or amph-conjugate gp100 vaccines, followed by adoptive transfer of CFSE-labeled Pmel-1 TCR-transgenic $CD8^+$ T cells that recognize the gp100 epitope (33) as reporters of antigen presentation. Pmel-1 T cells transferred 5 days post vaccination proliferated to a greater extent in the MLNs following amph-vaccination compared to soluble peptide immunization (Fig. 4A, B). More strikingly, Pmel-1 T cells transferred as late as two weeks after amph-gp100 immunization were still induced to undergo several rounds of cell division, while no reporter cell proliferation was detected in the MLNs of soluble peptide/CpG-immunized mice (Fig. 4C).

These data showed that amph-conjugates prolong antigen presentation in the MLN, but it was unclear if this was the dominant factor in responses to the conjugate vaccination, or if other potential effects (e.g., changes in which cells acquire antigen/adjuvant) could be important. To isolate the role of vaccine kinetics, we tested the impact of mimicking sustained antigen/adjuvant uptake in the amph-conjugate immunization by administering a simple soluble gag peptide/CpG vaccine as a bolus inoculation i.t. versus breaking up the

Author Manuscript Author Manuscript Author Manuscript Author Manuscript

dose into 5 injections administered every other day ("split" dosing, Fig. 4D). To differentiate the roles of peptide vs. adjuvant, we compared cohorts that received split peptide + bolus adjuvant or bolus peptide + split adjuvant dosing; the total dose of antigen and adjuvant received by each group was kept constant. As previously observed, bolus pulmonary peptide/CpG immunization elicited very low T-cell accumulation in the lungs (Fig. 4E, F). Split dosing of peptide combined with bolus CpG, or bolus peptide combined with split-dose CpG, were also ineffective. By contrast, split dosing of both antigen and adjuvant elicited a substantial antigen-specific T-cell population in lungs following a priming immunization, 70-fold greater than the split/bolus combinations (Fig. 4E, F).

To evaluate the impact of vaccine kinetics on the response to the booster immunization, we repeated these studies administering split or bolus dosing of vaccines at both prime and boost, and quantified T_{RM} formation in the lungs 30 days after the last dose (day 70, Fig. 4D). Bolus amph-conjugate vaccination was included as a comparator group. Similar to the post prime experiments, split-dosing of both peptide and adjuvant was the most effective regimen, eliciting 17-fold greater T-cell responses than split-dosed antigen + bolus adjuvant and 28-fold greater than bolus antigen + split-dosed adjuvant (Fig. 4G, H). Notably, the sustained antigen presentation achieved by bolus immunization with amph-conjugates led to similar levels of antigen-specific T_{RMs} as achieved by the optimal split-dosed vaccination. Similar to bolus amph-conjugate immunization, a majority of the lung-resident $CD8^+$ T cells elicited by split-dosed vaccination expressed CD69 and ~25% were $CD69^+CD103^+$ (fig. S7). Thus, T_{RM} establishment following mucosal vaccination is sensitive to both antigen and adjuvant kinetics, with prolonged exposure to both antigen and inflammatory cues promoting maximal resident memory establishment.

Amph-conjugates enhance T cell priming in MLNs at prime and directly in lung tissue at boost

Since amph-conjugates showed enhanced accumulation in both the lung parenchyma and MLNs relative to soluble vaccines, we next assessed whether i.t. vaccination primed T cells in the draining MLN, or alternatively, if T cells were expanded directly in the lung parenchyma. When mice were dosed with FTY720 daily starting 2 days before i.t. amph-conjugate vaccination, very few antigen-specific $CD8^+$ T cells were detected in the lung parenchyma at day 7 (Fig. 5A, B). Administration of amph-CpG alone did not recruit antigen-specific T cells to the lung regardless of FTY720 treatment. This suggested that initial T-cell priming occurs in the MLN, as observed in prior studies (34). To assess the location of T-cell activation at boosting, we primed groups of mice, then boosted the animals in the presence of FTY720 two weeks later. In this case, FTY720 treatment had no impact on the numbers of $CD8^+$ T cells accumulated in the lung parenchyma 7 days post boost (Fig. 5C, D), suggesting that the vaccine boost results in local antigen presentation and proliferation of $CD8^+$ T cells within the lung parenchyma, without a significant contribution of T cells trafficking from the circulation. This result was not due to a lack of antigen presentation in draining MLNs during the boost, because antigen-specific T cells were expanded in the MLNs (Fig. 5E). Similar to the post prime results, local inflammation induced by amph-CpG alone had no impact on lung T-cell accumulation (Fig. 5D). Thus,

Author Manuscript Author Manuscript Author Manuscript Author Manuscript

amph-vaccines can expand T cells directly in the lung tissue following booster immunization.

Amph-conjugate vaccines promote T_{RM} generation during booster immunization by recruitment and activation of cross-presenting DCs

Given the finding that trafficking of T cells from MLNs was not necessary for the expansion of T_{RMs} during boosting, we finally examined the effects of amph-conjugate and soluble peptide immunization on the key antigen presenting DC populations in the lungs. $CD103^+$ DCs and $CD11b^+$DCs were gated as previously described (fig. S8) (35). We found no appreciable increase in either the number of $CD11b^+$ or Batf3-dependent $CD103^+$ DCs in the lung parenchyma 6 days following primary immunization with soluble or amph-conjugates (Fig. 6A, B). Phenotyping lung Batf3-dependent $CD103^+$ DCs for surface expression of CD86 and MHC-II showed equivalent expression of activation markers in both soluble and amph-conjugate vaccinated mice (Fig. 6C, D). By contrast, at 6 days following administration of a booster immunization, we found that while soluble peptide vaccination again had no effect on DC populations in the lung tissue, amph-conjugate vaccination elicited a 3-fold increase in Batf3-dependent $CD103^+$ DCs (Fig. 6E). Interestingly, the number of lung $CD11b^+$ DCs in soluble- or amph-conjugate-vaccinated mice was significantly reduced compared to naïve mice at this time point (Fig. 6F). Approximately 30% of cross-presenting $CD103^+$ DCs in the lung expressed high levels of MHC-II and CD86 (Fig. 6G,H). These data suggest that boosting of T_{RM} expansion by pulmonary immunization with amph-conjugates is promoted by DC recruitment to the lung parenchyma.

Discussion

T_{RMs} play an important role in protection from pathogens and tumors at barrier tissues both in pre-clinical animal models (10, 36) and in humans (11, 37). Thus, strategies to promote T_{RM} generation at mucosal surfaces are of great interest for both cancer and infectious disease. Since vaccine efficacy is influenced by the anatomic location where immune responses are primed, one of the most effective strategies is to directly administer vaccines to mucosal surfaces (2, 9, 34). However, the natural barrier function of these tissues is an impediment to vaccination, e.g., in the lungs, where material is rapidly cleared to protect the airways. Here we exploited a natural transport pathway – bidirectional trafficking of albumin across the airway epithelium (23, 24) – as a strategy to enhance vaccination and induction of T_{RMs} in the lung parenchyma. Albumin further serves to promote subsequent trafficking to MLNs, following its natural trafficking pathway (20). Peptide antigens and CpG adjuvant modified with a phospholipid tail to promote binding to albumin exhibited increased accumulation and persistence in the lung parenchyma. These changes in vaccine pharmacokinetics correlated with 25-fold greater lung antigen-specific T-cell populations, which expressed markers of tissue residence. Consistent with the expectations for T_{RMs} in protective immunity, these responses correlated with enhanced protection from both pulmonary virus and tumor challenge.

Author Manuscript Author Manuscript Author Manuscript Author Manuscript

Vaccines targeting respiratory immunity often employ intranasal (i.n.) or aerosol immunization routes (the latter typically modeled by i.t. administration in rodents). Although intranasal administration is easily implemented clinically, i.n. immunization preferentially primes upper respiratory tract immunity and is less effective for lower respiratory tract antibody and T_{RM} responses (38). We confirmed these findings following rigorous i.n. vs. i.t. immunization with amph-vaccines. Small studies in human volunteers have also suggested that aerosol immunization reaching the lower respiratory tract is more immunogenic than i.n. immunization (39). Hence aerosol immunization may be desirable for more complete lung protection.

We previously showed that amph-conjugate peptide vaccines administered parenterally lead to much longer-lived antigen presentation compared to soluble peptide vaccines in draining lymph nodes (21). Similarly, here we found that amph-conjugate pulmonary immunization leads to antigen presentation persisting at least 13 days. Using simplified “split” dosing protocols with soluble peptide/adjuvant, we found that prolonged availability of both antigen and adjuvant is important for maximal T_{RM} induction in the lungs, and that sustained peptide/adjuvant availability in the MLNs and/or lung tissue appears to be the major factor governing the potency of amph-conjugate immunization. These data are consistent with prior reports suggesting that inflammatory stimuli must be coupled with pulmonary antigen to induce T_{RM} formation (40, 41). Additionally, several groups have demonstrated that continued viral antigen presentation influences the longevity and magnitude of both $CD4^+$(42) and $CD8^+$ (43) T_{RMs} in the context of pulmonary infection. Recently, Braeckel-Brudimir et al. showed that repeated antigen encounter through multiple rounds of infection increases the magnitude and durability of lung $CD8^+$ T_{RMs}, through increased seeding and improved survival of T cells within the lung (13).

Analysis of the impact of FTY720 treatment on amph-conjugate vaccine responses revealed that the vaccine mechanisms of action differ during prime vs. booster immunizations. Post prime, T cell activation in MLNs and homing to the lung tissue was required for establishment of lung-resident responses. This finding is consistent with studies showing that DCs in the MLN can imprint responding T cells with lung homing receptor expression (44). By contrast, during boosting, T-cell expansion was not impacted by blocking T-cell egress from lymphoid organs. This is in accordance with data from other groups who have observed that proliferation of antigen-primed $CD8^+$ T cells can occur in non-lymphoid tissues (34, 45).

Both soluble and amph-vaccination led to a reduction in $CD11b^+$ DCs post boost (Figure 6F). Although it is unclear why $CD11b^+$ DCs were reduced, the phenotype of myeloid cells in the lung is known to change with exposure to inflammatory stimuli (46, 47). Furthermore, the finding that amph-peptide immunization is entirely dependent on $Batf3^+$ dendritic cells (Fig. 2H) suggests that these cells do not play a significant role in antigen presentation after pulmonary amphiphile vaccination. Interestingly, amph-conjugate immunization both substantially expanded Batf3-dependent $CD103^+$ DCs in the lungs during boosting and induced greater DC activation. Thus, amph-conjugate immunization is able to enhance T-cell activation in draining lymph nodes and directly in the lung tissue, bolstering antigen presentation at both sites for effective responses during both the prime and boost.

Author Manuscript Author Manuscript Author Manuscript Author Manuscript

In conclusion, we have shown that mucosal immunization with amph-vaccines efficiently generates functional T_{RMs} in the lung, mediated by efficient uptake across the lung epithelium and prolonged antigen and adjuvant stimulation. Using amphiphile vaccines to generate robust mucosal immunity mediated by T_{RMs} could be beneficial in the context of prophylaxis for infectious diseases, the need for which has been underscored by the recent global coronavirus pandemic for which peptide vaccine platforms are actively being explored (48).

Materials and Methods

Study Design

The aims of this study were to characterize the immune response to amph-vaccines delivered into the lungs, to assess whether this form of vaccination could protect from virus or tumor challenges, and define mechanisms of action for this vaccine. T cells in the lung were enumerated by flow cytometry following standard protocols. To study the functional efficacy of T cells generated in the lung, mice were infected intra-tracheally with lethal doses of vaccinia virus expressing a defined antigen. For tumor studies, melanoma cells were introduced into the lung by intravenous injection. All animal experiments were repeated at least twice with $n = 2–10$ animals/group being studied. No outliers were excluded from the data analyses and studies were not blinded.

Materials

Peptides with an N-terminal cysteine (AL11: CAAVKNWMTQTL, gp100: CAVGALEGPRNQDWLGVPRQL, Trp1: CTAPDNLGYM, Trp2: CSVYDFFVWL) (26, 49) were ordered from Genscript, NJ and conjugation to maleimide-PEG-DSPE amphiphiles was performed as previously described (20, 21). Amphiphile-conjugated CpG (Amph-CpG) was produced by solid-phase synthesis of Class B CpG 1826 oligonucleotide with a G_2 spacer conjugated to an 18-carbon diacyl tail via the 5’ end as previously described (20).

Animals

All mice were purchased from The Jackson Laboratory. Vaccination experiments were performed in 6–8 week old WT C57BL/6 mice (Strain number: 000664), *FcRn*$^{-/-}$ (Strain number: 003982) and *Batf3*$^{-/-}$ mice (Strain number: 013755). Tumor studies were performed in albino C57BL/6 mice (Strain number: 000058). For T cell adoptive transfer experiments gp100-specific T cells were isolated from B6.Cg-*Thy1*^{a}/Cy Tg(TcraTcrb)8Rest/J Pmel-1 transgenic mice (Strain number: 005023). All experiments were performed in accordance with NIH ethical guidelines following an Institutional Animal Care and Use Committee-approved protocol.

Vaccinations

Mice were immunized with peptide and CpG either in their soluble or amph-conjugate forms at indicated doses. Intratracheal administration was performed using a platform and light source to visualize the tracheal opening of an anesthetized mouse and instill up to 50 μl of vaccine solution or 10^6 pfu of vaccinia virus as described (50). Subcutaneous vaccination was performed at the base of the tail.

Author Manuscript Author Manuscript Author Manuscript Author Manuscript

Vaccinia Challenge

Four months after vaccine boosting, mice were infected intratracheally with vaccinia virus expressing the AL11 epitope from SIV gag (10^6 pfu per mouse) (50). Animal weights were recorded daily post challenge and animals were euthanized when their weight decreased by > 20%. To quantify viral titers, lung tissue homogenates were used to infect CV-1 cells in culture and resulting plaques were quantified (51). Mice were also treated with 1 mg/kg FTY720 (or vehicle control) delivered daily by intraperitoneal injection beginning 5 days prior to vaccinia infection.

Tumor Studies

100,000 or 400,000 B16F10 cells that were transduced with GFP and luciferase were injected intravenously to seed melanoma tumors in the lungs. When used, anti-PD1 was administered intra-peritoneally at 200 mg/kg every 3 days. Tumor growth was monitored by bioluminescence imaging using an IVIS Spectrum imager and mice were sacrificed when the average radiance or ROIs over the lungs of animals exceeded $5X10^6$ photons/s/cm^2/sr.

Adoptive Transfer

$CD8^+$ T cells were isolated from spleens of Pmel-1 transgenic mice by negative selection using an EasySep mouse $CD8^+$ T cell isolation kit (Stemcell Technologies, MA). T cells were labeled with CFSE and 500,000 cells were injected retro-orbitally followed by sacrifice 2 days later and recovery of mediastinal lymph nodes for analysis of CFSE dilution in Pmel-1 T cells by flow cytometry.

Flow Cytometry

Lungs, mediastinal lymph nodes and peripheral blood were collected from immunized and control animals. Lung lobes were separated and cut into small pieces in PBS containing 0.5% FBS and 0.05M HEPES buffer with 120U/ml Collagenase IV (Worthington Bio, NJ) and 40 U/m DNase I (bioWorld, OH). Single cell suspensions were made using the gentleMACS lung dissociation protocol (52). Mediastinal lymph nodes were passed through a 70 μm cell strainer to obtain a single cell suspension of lymphocytes. Red blood cells were lysed using ACK lysis buffer (Gibco, MD). Single cell suspensions were washed with PBS and re-suspended in flow cytometry staining buffer (PBS+2% FBS+0.1% sodium azide). Cells were stained with fluorescently labeled antibodies and tetramers and samples were analyzed on LSR Fortessa or Canto (Becton Dickinson, NJ) flow cytometry instruments. Data were analyzed using FlowJo (TreeStar). Antibodies used were the following: anti-CD8α (53–6.7), anti-CD69 (H1.2F3), anti-CD103 (2E7), anti-TNFα (MPX-XT22), anti-IFNγ (XMG1.2), anti-CD11a (H155–78), anti-CD49a (Hα31/8), anti-CD11c (N418), anti-CD11b (M1/70), anti-CD24 (M1/69), anti-CD64 (X54–5/7.1), anti-SiglecF (1RNM44N) and anti-CD45 (30-F11). $CD103^+$ DCs and $CD11b^+$ DCs in the lung were identified by using a previously established gating scheme (fig. S8) (53).

Immunofluorescence

Lungs from immunized or control mice were isolated, fixed in periodate-lysine-paraformaldehyde (PLP) buffer and inflated with 2 ml of a mixture of equal parts PBS and

Author Manuscript Author Manuscript Author Manuscript Author Manuscript

optimum cutting temperature (OCT) compound as described (52). Inflated lungs were embedded in OCT and frozen. Cryosections were cut and stained with DAPI. Images were acquired using a 30X objective on an Olympus FV1200 laser scanning confocal microscope. Image analysis was performed using ImageJ (NIH).

Statistical Analysis

Sample sizes were chosen based on known effect sizes of amph-conjugate immunization in prior work (20, 21) and pilot experiments. Statistical analyses were performed using GraphPad Prism version 8. Analysis of multiple groups was performed using one-way or two-way ANOVA using the Tukey post hoc test for multiple comparison within groups. Graphs indicate the mean and standard error of the mean (SEM) for the various groups. $p<0.05$ was considered to be statistically significant.

Supplementary Material

Refer to Web version on PubMed Central for supplementary material.

Acknowledgments

We thank the Koch Institute Swanson Biotechnology Center for technical support, specifically the flow cytometry and microscopy facilities. We thank Peter Choi for reviewing and editing this manuscript.

Funding:

This work was supported by the following grants: The Bridge Project, a partnership between the Koch Institute at MIT and the Dana-Farber/ Harvard Cancer Center, the Marble Center for Cancer Nanomedicine, the Ragon Institute of MGH, MIT, and Harvard, and the NIH (awards EB022433 and CA247632). KR was funded by a Koch Institute Quinquennial fellowship. DJI is an investigator of the Howard Hughes Medical Institute.

References

1. Wu T, Hu Y, Lee Y-TY-T, Bouchard KR, Benechet A, Khanna K, Cauley LS, Lung-resident memory CD8 T cells (TRM) are indispensable for optimal cross-protection against pulmonary virus infection. J. Leukoc. Biol. 95, 215–24 (2014). [PubMed: 24006506]
2. Perdomo C, Zedler U, Kühl AA, Lozza L, Saikali P, Sander LE, Vogelzang A, Kaufmann SHE, Kupz A, Mucosal BCG Vaccination Induces Protective Lung-Resident Memory T Cell Populations against Tuberculosis. MBio. 7, e01686–16 (2016). [PubMed: 27879332]
3. Tan HX, Wheatley AK, Esterbauer R, Jegaskanda S, Glass JJ, Masopust D, De Rose R, Kent SJ, Induction of vaginal-resident HIV-specific CD8 T cells with mucosal prime-boost immunization. Mucosal Immunol. 11, 994–1007 (2018). [PubMed: 29067995]
4. Schenkel JM, Fraser KA, Vezys V, Masopust D, Sensing and alarm function of resident memory CD8+ T cells. Nat. Immunol. 14, 509–513 (2013). [PubMed: 23542740]
5. Schenkel JM, Fraser KA, Beura LK, Pauken KE, Vezys V, Masopust D, T cell memory. Resident memory CD8 T cells trigger protective innate and adaptive immune responses. Science. 346, 98–101 (2014). [PubMed: 25170049]
6. Purwar R, Campbell J, Murphy G, Richards WG, Clark RA, Kupper TS, Resident Memory T cells (TRM) are abundant in human lung: Diversity, function, and antigen specificity. PLoS One. 6, 16245 (2011).
7. Turner DL, Bickham KL, Thome JJ, Kim CY, D'Ovidio F, Wherry EJ, Farber DL, Lung niches for the generation and maintenance of tissue-resident memory T cells. Mucosal Immunol. 7, 501–10 (2014). [PubMed: 24064670]

Author Manuscript Author Manuscript Author Manuscript Author Manuscript

8. Pallett LJ, Davies J, Colbeck EJ, Robertson F, Hansi N, Easom NJW, Burton AR, Stegmann KA, Schurich A, Swadling L, Gill US, Male V, Luong TV, Gander A, Davidson BR, Kennedy PTF, Maini MK, IL-2high tissue-resident T cells in the human liver: Sentinels for hepatotropic infection. J. Exp. Med. 214, 1567–1580 (2017). [PubMed: 28526759]
9. Sandoval F, Terme M, Nizard M, Badoual C, Bureau M-F, Freyburger L, Clement O, Marcheteau E, Gey A, Fraisse G, Bouguin C, Merillon N, Dransart E, Tran T, Quintin-Colonna F, Autret G, Thiebaud M, Suleman M, Riffault S, Wu T-C, Launay O, Danel C, Taieb J, Richardson J, Zitvogel L, Fridman WH, Johannes L, Tartour E, Mucosal Imprinting of Vaccine-Induced CD8+ T Cells Is Crucial to Inhibit the Growth of Mucosal Tumors. Sci. Transl. Med. 5, 172ra20–172ra20 (2013).
10. Nizard M, Roussel H, Diniz MO, Karaki S, Tran T, Voron T, Dransart E, Sandoval F, Riquet M, Rance B, Marcheteau E, Fabre E, Mandavit M, Terme M, Blanc C, Escudie J-B, Gibault L, Barthes FLP, Granier C, Ferreira LCS, Badoual C, Johannes L, Tartour E, Induction of resident memory T cells enhances the efficacy of cancer vaccine. Nat. Commun. 8, 15221 (2017). [PubMed: 28537262]
11. Ganesan A-P, Clarke J, Wood O, Garrido-Martin EM, Chee SJ, Mellows T, Samaniego-Castruita D, Singh D, Seumois G, Alzetani A, Woo E, Friedmann PS, V King E, Thomas GJ, Sanchez-Elsner T, Vijayanand P, Ottensmeier CH, Tissue-resident memory features are linked to the magnitude of cytotoxic T cell responses in human lung cancer. Nat. Immunol. 18, 940–950 (2017). [PubMed: 28628092]
12. Bergsbaken T, Bevan MJ, Fink PJ, Local Inflammatory Cues Regulate Differentiation and Persistence of CD8+ Tissue-Resident Memory T Cells. Cell Rep. 19, 114–124 (2017). [PubMed: 28380351]
13. Van Braeckel-Budimir N, Varga SM, Badovinac VP, Harty Correspondence JT, Harty JT, Repeated Antigen Exposure Extends the Durability of Influenza-Specific Lung-Resident Memory CD8+ T Cells and Heterosubtypic Immunity. Cell Rep. 24, 3374–3382 (2018). [PubMed: 30257199]
14. Zhang N, Bevan MJ, Transforming growth factor-β signaling controls the formation and maintenance of gut-resident memory T cells by regulating migration and retention. Immunity. 39, 687–696 (2013). [PubMed: 24076049]
15. Milner JJ, Toma C, Yu B, Zhang K, Omilusik K, Phan AT, Wang D, Getzler AJ, Nguyen T, Crotty S, Wang W, Pipkin ME, Goldrath AW, Runx3 programs CD8+ T cell residency in non-lymphoid tissues and tumours. Nature. 552, 253–257 (2017). [PubMed: 29211713]
16. Li W, Joshi MD, Singhania S, Ramsey KH, Murthy AK, Peptide vaccine: Progress and challenges. Vaccines. 2 (2014), pp. 515–536. [PubMed: 26344743]
17. Bezu L, Kepp O, Cerrato G, Pol J, Fucikova J, Spisek R, Zitvogel L, Kroemer G, Galluzzi L, Trial watch: Peptide-based vaccines in anticancer therapy. Oncoimmunology. 7 (2018), doi:110.1080/2162402X.2018.1511506.
18. Melief CJM, van Hall T, Arens R, Ossendorp F, van der Burg SH, Therapeutic cancer vaccines. J. Clin. Invest. 125, 1–12 (2015). [PubMed: 25654544]
19. Inoue N, Abe M, Kobayashi R, Yamada S, in Advances in Experimental Medicine and Biology (Springer New York LLC, 2018), vol. 1045, pp. 271–296. [PubMed: 29896672]
20. Liu H, Moynihan KD, Zheng Y, Szeto GL, V Li A, Huang B, Van Egeren DS, Park C, Irvine DJ, Structure-based programming of lymph-node targeting in molecular vaccines. Nature. 507, 519–22 (2014). [PubMed: 24531764]
21. Moynihan KD, Holden RL, Mehta NK, Wang C, Karver MR, Dinter J, Liang S, Abraham W, Melo MB, Zhang AQ, Li N, Le Gall S, Pentelute BL, Irvine DJ, Enhancement of Peptide Vaccine Immunogenicity by Increasing Lymphatic Drainage and Boosting Serum Stability. Cancer Immunol. Res. 6, 1025–1038 (2018). [PubMed: 29915023]
22. Ma L, Dichwalkar T, Chang JYH, Cossette B, Garafola D, Zhang AQ, Fichter M, Wang C, Liang S, Silva M, Kumari S, Mehta NK, Abraham W, Thai N, Li N, Dane Wittrup K, Irvine DJ, Enhanced CAR–T cell activity against solid tumors by vaccine boosting through the chimeric receptor. Science (80-.). 365, 162–168 (2019).
23. Sand KMK, Bern M, Nilsen J, Noordzij HT, Sandlie I, Andersen JT, Unraveling the interaction between FcRn and albumin: opportunities for design of albumin-based therapeutics. Front. Immunol. 5 (2014), doi:10.3389/fimmu.2014.00682.

Author Manuscript Author Manuscript Author Manuscript Author Manuscript

24. Anderson CL, Chaudhury C, Kim J, Bronson CL, Wani MA, Mohanty S, Perspective-- FcRn transports albumin: relevance to immunology and medicine. Trends Immunol. 27, 343–8 (2006). [PubMed: 16731041]
25. Kantrow SP, Shen Z, Jagneaux T, Zhang P, Nelson S, Neutrophil-mediated lung permeability and host defense proteins. Am. J. Physiol. Lung Cell. Mol. Physiol. 297, L738–45 (2009). [PubMed: 19648288]
26. Barouch DH, Pau MG, Custers JHHV, Koudstaal W, Kostense S, Havenga MJE, Truitt DM, Sumida SM, Kishko MG, Arthur JC, Korioth-Schmitz B, Newberg MH, Gorgone DA, Lifton MA, Panicali DL, Nabel GJ, Letvin NL, Goudsmit J, Immunogenicity of Recombinant Adenovirus Serotype 35 Vaccine in the Presence of Pre-Existing Anti-Ad5 Immunity. J. Immunol. 172, 6290–6297 (2004). [PubMed: 15128818]
27. Anderson KG, Sung H, Skon CN, Lefrancois L, Deisinger A, Vezys V, Masopust D, Cutting edge: intravascular staining redefines lung CD8 T cell responses. J. Immunol. 189, 2702–6 (2012). [PubMed: 22896631]
28. Ray SJ, Franki SN, Pierce RH, Dimitrova S, Koteliansky V, Sprague AG, Doherty PC, de Fougerolles AR, Topham DJ, The Collagen Binding α1β1 Integrin VLA-1 Regulates CD8 T Cell-Mediated Immune Protection against Heterologous Influenza Infection. Immunity. 20, 167–179 (2004). [PubMed: 14975239]
29. Cyster JG, Schwab SR, Sphingosine-1-Phosphate and Lymphocyte Egress from Lymphoid Organs. Annu. Rev. Immunol. 30, 69–94 (2012). [PubMed: 22149932]
30. MacKay LK, Rahimpour A, Ma JZ, Collins N, Stock AT, Hafon ML, Vega-Ramos J, Lauzurica P, Mueller SN, Stefanovic T, Tscharke DC, Heath WR, Inouye M, Carbone FR, Gebhardt T, The developmental pathway for CD103+ CD8+ tissue-resident memory T cells of skin. Nat. Immunol. 14, 1294–1301 (2013). [PubMed: 24162776]
31. Mackay LK, Wynne-Jones E, Freestone D, Pellicci DG, Mielke LA, Newman DM, Braun A, Masson F, Kallies A, Belz GT, Carbone FR, T-box Transcription Factors Combine with the Cytokines TGF-β and IL-15 to Control Tissue-Resident Memory T Cell Fate. Immunity. 43, 1101–1111 (2015). [PubMed: 26682984]
32. Adachi K, Chiba K, FTY720 story. Its discovery and the following accelerated development of sphingosine 1-phosphate receptor agonists as immunomodulators based on reverse pharmacology. Perspect. Medicin. Chem. 1, 11–23 (2007). [PubMed: 19812733]
33. Overwijk WW, Theoret MR, Finkelstein SE, Surman DR, de Jong LA, Vyth-Dreese FA, Dellemijn TA, Antony PA, Spiess PJ, Palmer DC, Heimann DM, Klebanoff CA, Yu Z, Hwang LN, Feigenbaum L, Kruisbeek AM, Rosenberg SA, Restifo NP, Tumor Regression and Autoimmunity after Reversal of a Functionally Tolerant State of Self-reactive CD8 $^{+}$ T Cells. J. Exp. Med. 198, 569–580 (2003). [PubMed: 12925674]
34. Çuburu N, Graham BS, Buck CB, Kines RC, Pang Y-YS, Day PM, Lowy DR, Schiller JT, Intravaginal immunization with HPV vectors induces tissue-resident CD8+ T cell responses. J. Clin. Invest. 122, 4606–20 (2012). [PubMed: 23143305]
35. Misharin AV, Morales-Nebreda L, Mutlu GM, Budinger GRS, Perlman H, Flow cytometric analysis of macrophages and dendritic cell subsets in the mouse lung. Am. J. Respir. Cell Mol. Biol. 49, 503–510 (2013). [PubMed: 23672262]
36. Schenkel JM, Masopust D, Tissue-resident memory T cells. Immunity. 41, 886–97 (2014). [PubMed: 25526304]
37. Piet B, de Bree GJ, Smids-Dierdorp BS, van der Loos CM, Remmerswaal EBM, von der Thüsen JH, van Haarst JMW, Eerenberg JP, ten Brinke A, van der Bij W, Timens W, van Lier RAW, Jonkers RE, CD8+ T cells with an intraepithelial phenotype upregulate cytotoxic function upon influenza infection in human lung. J. Clin. Invest. 121, 2254–2263 (2011). [PubMed: 21537083]
38. Sanders MT, Deliyannis G, Pearse MJ, McNamara MK, Brown LE, Single dose intranasal immunization with ISCOMATRIX™ vaccines to elicit antibody-mediated clearance of influenza virus requires delivery to the lower respiratory tract. Vaccine. 27, 2475–2482 (2009). [PubMed: 19368789]
39. Nardelli-Haefliger D, Lurati F, Wirthner D, Spertini F, Schiller JT, Lowy DR, Ponci F, De Grandi P, Immune responses induced by lower airway mucosal immunisation with a human

Author Manuscript Author Manuscript Author Manuscript Author Manuscript

papillomavirus type 16 virus-like particle vaccine. Vaccine. 23, 3634–3641 (2005). [PubMed: 15882523]

40. Takamura S, Yagi H, Hakata Y, Motozono C, McMaster SR, Masumoto T, Fujisawa M, Chikaishi T, Komeda J, Itoh J, Umemura M, Kyusai A, Tomura M, Nakayama T, Woodland DL, Kohlmeier JE, Miyazawa M, Specific niches for lung-resident memory CD8+ T cells at the site of tissue regeneration enable CD69-independent maintenance. J. Exp. Med. 213, 3057–3073 (2016). [PubMed: 27815325]
41. McMaster SR, Wein AN, Dunbar PR, Hayward SL, Cartwright EK, Denning TL, Kohlmeier JE, Pulmonary antigen encounter regulates the establishment of tissue-resident CD8 memory T cells in the lung airways and parenchyma article. Mucosal Immunol. 11, 1071–1078 (2018). [PubMed: 29453412]
42. Jelley-Gibbs DM, Brown DM, Dibble JP, Haynes L, Eaton SM, Swain SL, Unexpected prolonged presentation of influenza antigens promotes CD4 T cell memory generation. J. Exp. Med. 202, 697–706 (2005). [PubMed: 16147980]
43. Kim TS, Hufford MM, Sun J, Fu YX, Braciale TJ, Antigen persistence and the control of local T cell memory by migrant respiratory dendritic cells after acute virus infection. J. Exp. Med. 207, 1161–1172 (2010). [PubMed: 20513748]
44. Mikhak Z, Strassner JP, Luster AD, Lung dendritic cells imprint T cell lung homing and promote lung immunity through the chemokine receptor CCR4. J. Exp. Med. 210, 1855–69 (2013). [PubMed: 23960189]
45. Stary G, Olive A, Radovic-Moreno AF, Gondek D, Alvarez D, Basto PA, Perro M, Vrbanac VD, Tager AM, Shi J, Yethon JA, Farokhzad OC, Langer R, Starnbach MN, von Andrian UH, VACCINES. A mucosal vaccine against Chlamydia trachomatis generates two waves of protective memory T cells. Science. 348, aaa8205 (2015). [PubMed: 26089520]
46. Ginhoux F, Schlitzer A, CD11b+ DCs rediscovered: Implications for vaccination. Expert Rev. Vaccines. 13 (2014), pp. 445–447. [PubMed: 24564769]
47. Desch AN, Henson PM, V Jakubzick C, Pulmonary dendritic cell development and antigen acquisition. Immunol. Res. 55, 178–86 (2013). [PubMed: 22968708]
48. Wang N, Shang J, Jiang S, Du L, Subunit Vaccines Against Emerging Pathogenic Human Coronaviruses. Front. Microbiol. 11 (2020), doi:10.3389/fmicb.2020.00298.
49. Moynihan KDKD, Opel CFCF, Szeto GLGL, Tzeng A, Zhu EFEF, Engreitz JMJM, Williams RTRT, Rakhra K, Zhang MHMH, Rothschilds AMAM, Kumari S, Kelly RLRL, Kwan BHBH, Abraham W, Hu K, Mehta NKNK, Kauke MJMJ, Suh H, Cochran JRJR, Lauffenburger DADA, Wittrup KDD, Irvine DJDJ, Eradication of large established tumors in mice by combination immunotherapy that engages innate and adaptive immune responses. Nat Med. 22, 1402–1410 (2016). [PubMed: 27775706]
50. Suh H, Elkhader J, Seidman MA, Abraham W, Im E-J, Irvine DJ, Barouch DH, Foley MH, Yen M, Moon JJ, Li AV, Generation of Effector Memory T Cell-Based Mucosal and Systemic Immunity with Pulmonary Nanoparticle Vaccination. Sci. Transl. Med. 5, 204ra130–204ra130 (2013).
51. Nakaya Y, Zheng H, García-Sastre A, Enhanced cellular immune responses to SIV Gag by immunization with influenza and vaccinia virus recombinants. Vaccine. 21, 2097–106 (2003). [PubMed: 12706700]
52. Joshi NS, Akama-Garren EH, Lu Y, Lee D-Y, Chang GP, Li A, DuPage M, Tammela T, Kerper NR, Farago AF, Robbins R, Crowley DM, Bronson RT, Jacks T, Regulatory T Cells in Tumor-Associated Tertiary Lymphoid Structures Suppress Anti-tumor T Cell Responses. Immunity. 43, 579–90 (2015). [PubMed: 26341400]
53. V Misharin A, Morales-Nebreda L, Mutlu GM, Budinger GRS, Perlman H, Flow cytometric analysis of macrophages and dendritic cell subsets in the mouse lung. Am. J. Respir. Cell Mol. Biol. 49, 503–10 (2013). [PubMed: 23672262]

Author Manuscript Author Manuscript Author Manuscript Author Manuscript

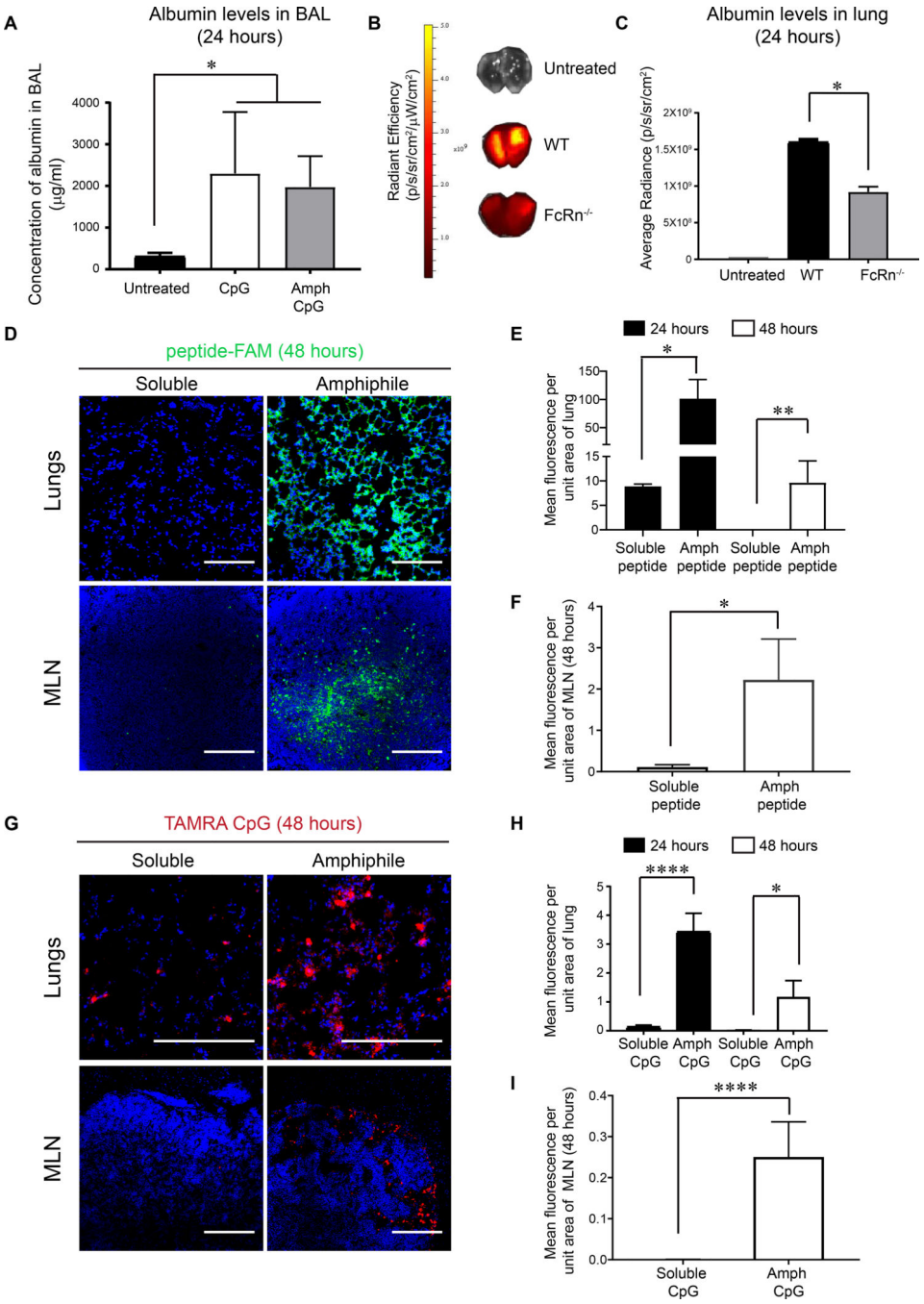

Figure 1. Amphiphile peptides or CpG are retained in the lung parenchyma and draining MLNs.

(**A**) Albumin levels measured by ELISA in bronchoalveolar lavage (BAL) from WT mice that were untreated or treated with inflammatory stimuli i.t. (**B**) Labeled mouse albumin was delivered i.t. into WT and FcRn$^{-/-}$ mice (n = 3/group) and fluorescence signal from lungs was measured by IVIS imaging 24 hours later. (**C**) Quantification of fluorescence signal from experiment described in (B). (**D-I**) C57BL/6 mice (n=3/group) were administered 20 μg FAM-labeled (green) gp100 peptide, an equimolar amount of labeled amph-gp100, 10 μg TAMRA-labeled (red) CpG, or an equimolar amount of labeled amph-CpG. Shown are

Author Manuscript Author Manuscript Author Manuscript Author Manuscript

representative immunofluorescence images of lungs (upper panel, scale bar = 100 μm in D and 200 μm in G) and MLNs (lower panel, scale bar = 100 μm) harvested from mice at 48 hours post immunization (D, G; DAPI (blue) was used to stain nuclei). Quantification of peptide or CpG signals from the lungs at 24 and 48 hours are shown in (**E**, **H**) and MLNs (**F**, **I**). Data shown are mean ± SEM, *p<0.05, **p<0.001, ****p<0.0001 as determined by one-way ANOVA. Data are representative of at least two independent experiments.

Author Manuscript Author Manuscript Author Manuscript Author Manuscript

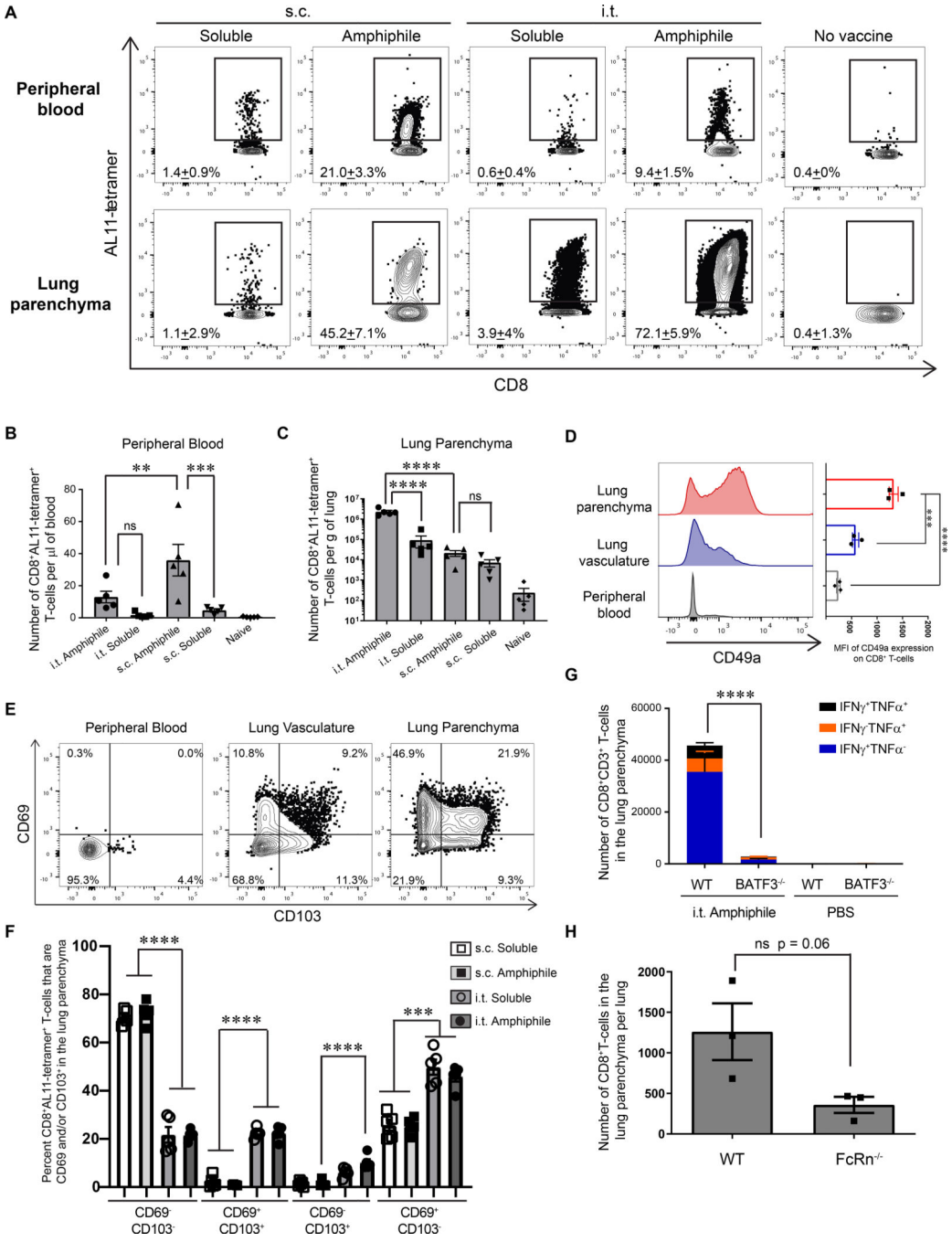

Figure 2: Mucosal amph-vaccines elicit robust expansion of antigen-specific CD8$^+$ T_{RMs} in the lungs.

C57BL/6 mice were immunized either s.c. or i.t. with 5 µg of free AL11 peptide and 8 µg CpG or equimolar doses of amph-AL11 combined with amph-CpG on days 0 and 14. **(A)** Representative flow cytometry plots of CD8$^+$AL11-tetramer$^+$ T cells in the blood (upper panel) and lung parenchyma (lower panel) at day 20. **(B, C)** Quantification of CD8$^+$AL11-tetramer$^+$ cells in the blood (B) and lung parenchyma (C). **(D)** Representative histograms of CD49a expression on CD8$^+$ T cells and quantification of CD49a mean fluorescence intensity

Author Manuscript Author Manuscript Author Manuscript Author Manuscript

(MFI) following i.t. amph-vaccination. **(E)** Representative flow cytometry plots of CD69 and CD103 expression on $CD8^+$AL11-$tetramer^+$ T cells in the blood (left panel), lung vasculature (center panel) and lung parenchyma (right panel) following i.t. amph-vaccination. **(F)** Quantification of the percentage of lung $CD8^+$AL11-$tetramer^+$ T cells expressing CD69, CD103 or both. **(G)** WT and *Batf3*$^{-/-}$ mice were vaccinated with amph-gp100 and amph-CpG i.t. following the schedule in (A). Quantification of $cytokine^+$ $CD8^+$ lung T cells. **(H)** WT and $FcRn^{-/-}$ mice were vaccinated with amph-gp100 and amph-CpG i.t. following the schedule in (A) and lung antigen-specific $CD8^+$ T cells were quantified. Data are shown are mean ± SEM, **p<0.01, ***p<0.001, ****p<0.0001 as determined by one-way ANOVA. Data are representative of at least three independent experiments (n = 3 – 5 animals/group).

Author Manuscript Author Manuscript Author Manuscript Author Manuscript

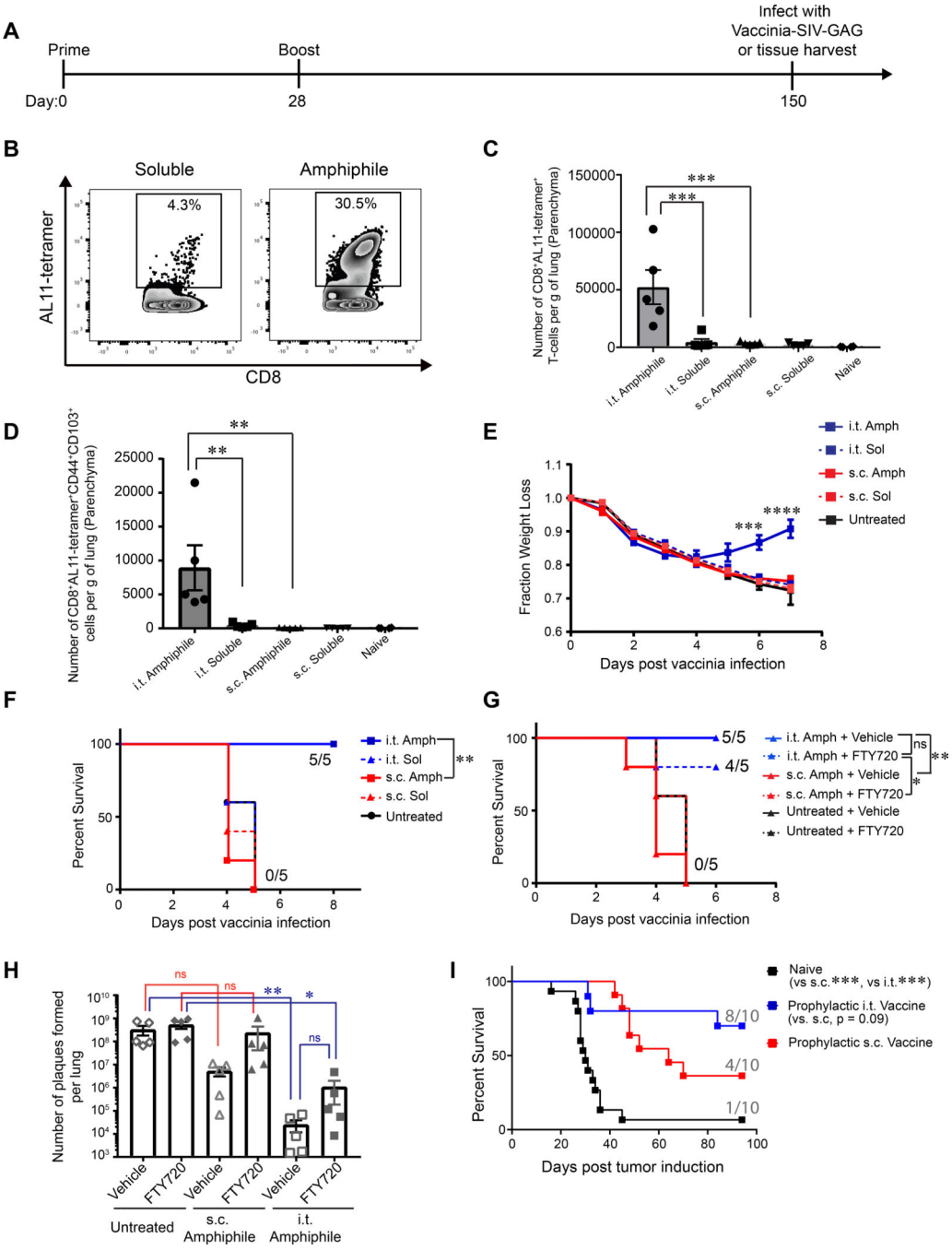

Figure 3: Antigen-specific CD8$^+$ T cells elicited by i.t. amph-vaccination are long-lived and protect from viral challenge.

(A) C57BL/6 mice (n=5/group) were vaccinated with 5 μg AL11 peptide combined with 8 μg CpG or equimolar doses of amph-AL11 and amph-CpG administered i.t. or s.c. on days 0 and 28, and then challenged with a lethal dose of SIV-Gag vaccinia virus (10^6 pfu) i.t. or sacrificed to characterize the immune response in the lungs on day 150. **(B)** Representative flow cytometry plots of CD8$^+$AL11-tetramer$^+$ T cells in the lung parenchyma. **(C)** Enumeration of lung CD8$^+$AL11-tetramer$^+$ T cells at day 150. **(D)** Enumeration of

Author Manuscript Author Manuscript Author Manuscript Author Manuscript

$CD44^+CD103^+CD8^+AL11\text{-tetramer}^+$ T cells at day 150. (**E, F**) Animal weights over time (E) and survival (F) post vaccinia virus challenge. **(G, H)** C57BL/6 mice (n=5/group) were left naïve or vaccinated as in (A), then challenged with vaccinia virus at day 150 in the presence or absence of FTY720. Shown is overall survival (G) and number of viral plaques in the lungs at day 6 post challenge (H). **(I)** C57BL/6 mice (n=10/group) were left naïve or vaccinated with 10 μg gp100, 10 μg Trp1, and 10 μg Trp2 peptide antigens combined with 8 μg CpG, or vaccinated with equimolar doses of amph-peptides and amph-CpG on days 0 and 14. Thirty days post boost mice were challenged with 4×10^5 B16F10 melanoma cells i.v. and survival over time is plotted. In each cohort the number of mice surviving at 80 days is indicated. Data are represented as mean ± SEM, from three independent experiments (A-H) and two independent experiments (I), *p<0.01, **p < 0.001, ***p<0.0001; ****p<0.00001; ns, not significant. Survival data were analyzed using a log rank test and comparisons between multiple groups were performed using one-way ANOVA.

Author Manuscript Author Manuscript Author Manuscript Author Manuscript

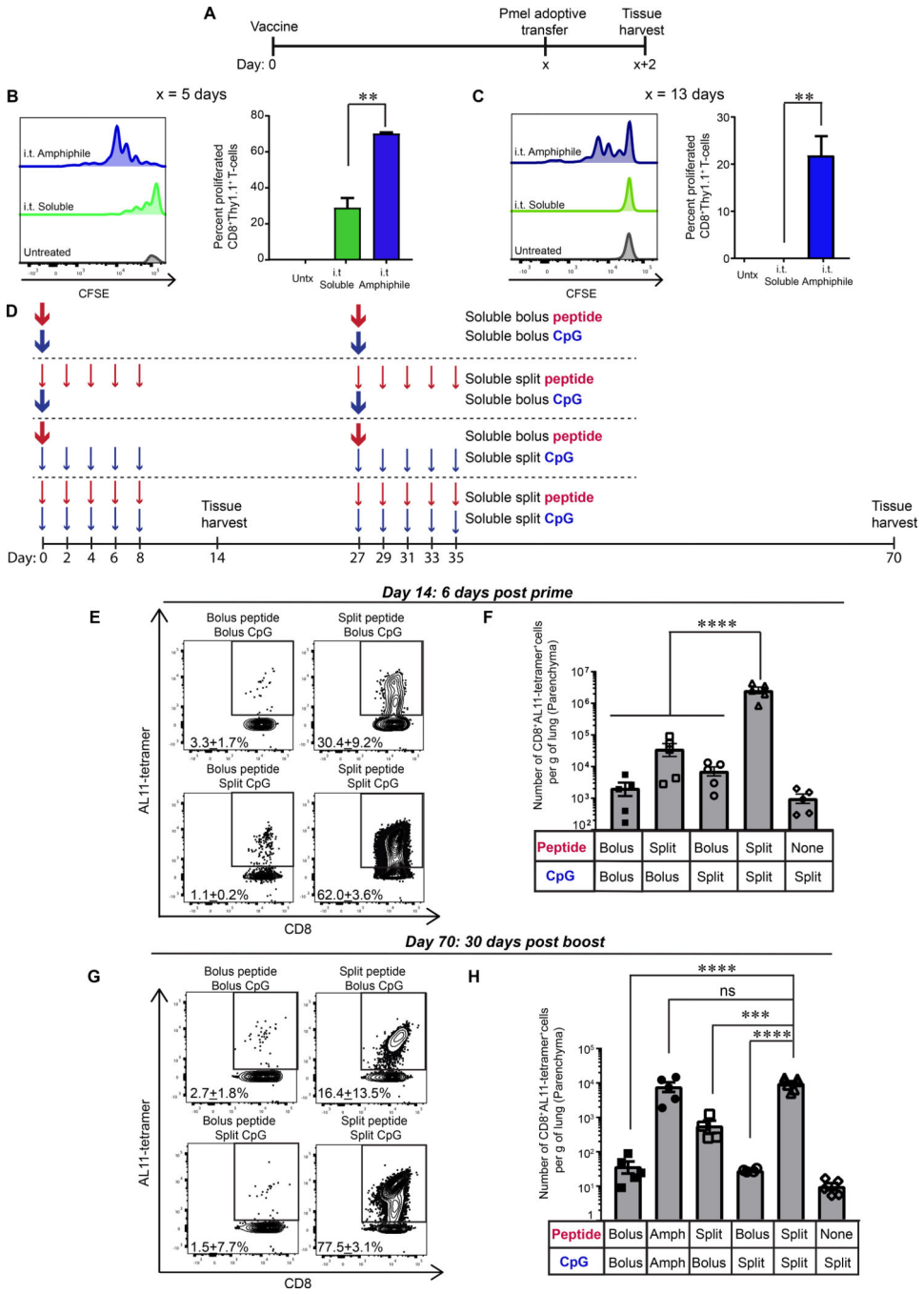

Figure 4: Extended exposure to both antigen and adjuvant promotes T_{RM} development.

(A-C) C57BL/6 mice were vaccinated on day 0 with 10 μg gp100 and 8 μg CpG or equimolar doses of amph-gp100 and amph-CpG. At 5 or 13 days later, 5×10^5 CFSE-labeled Pmel-1 $CD8^+$ T cells were adoptively transferred, and tissues were harvested 48 hours later for flow cytometry analysis. Shown are the experiment timeline (A), and representative histograms of CFSE dilution and percent of divided Pmel-1 T cells derived from MLNs (n = 4/group) of mice that received adoptive transfer on day 5 (B) or day 13 (C). **(D-H)** C57BL/6 mice (*n* = 5–7/group) were immunized with soluble AL11 peptide and CpG following the

Author Manuscript Author Manuscript Author Manuscript Author Manuscript

dosing patterns indicated. The total dose for each regimen was fixed at 10 μg AL11 and 8 μg CpG. Tissues were harvested on day 14 post prime or 35 days post boost on day 70. Shown are the dosing schedules (D), representative flow cytometry plots of lung $CD8^+$AL11-tetramer$^+$ T cells on day 14 post prime (E) or day 70 post boost (G), and enumeration of tetramer$^+$ T cells on day 14 (F) and day 70 (H). Data are shown are mean ± SEM, ***p<0.001, ****p<0.0001 as determined by one-way ANOVA. Data are representative of three independent experiments.

Author Manuscript Author Manuscript Author Manuscript Author Manuscript

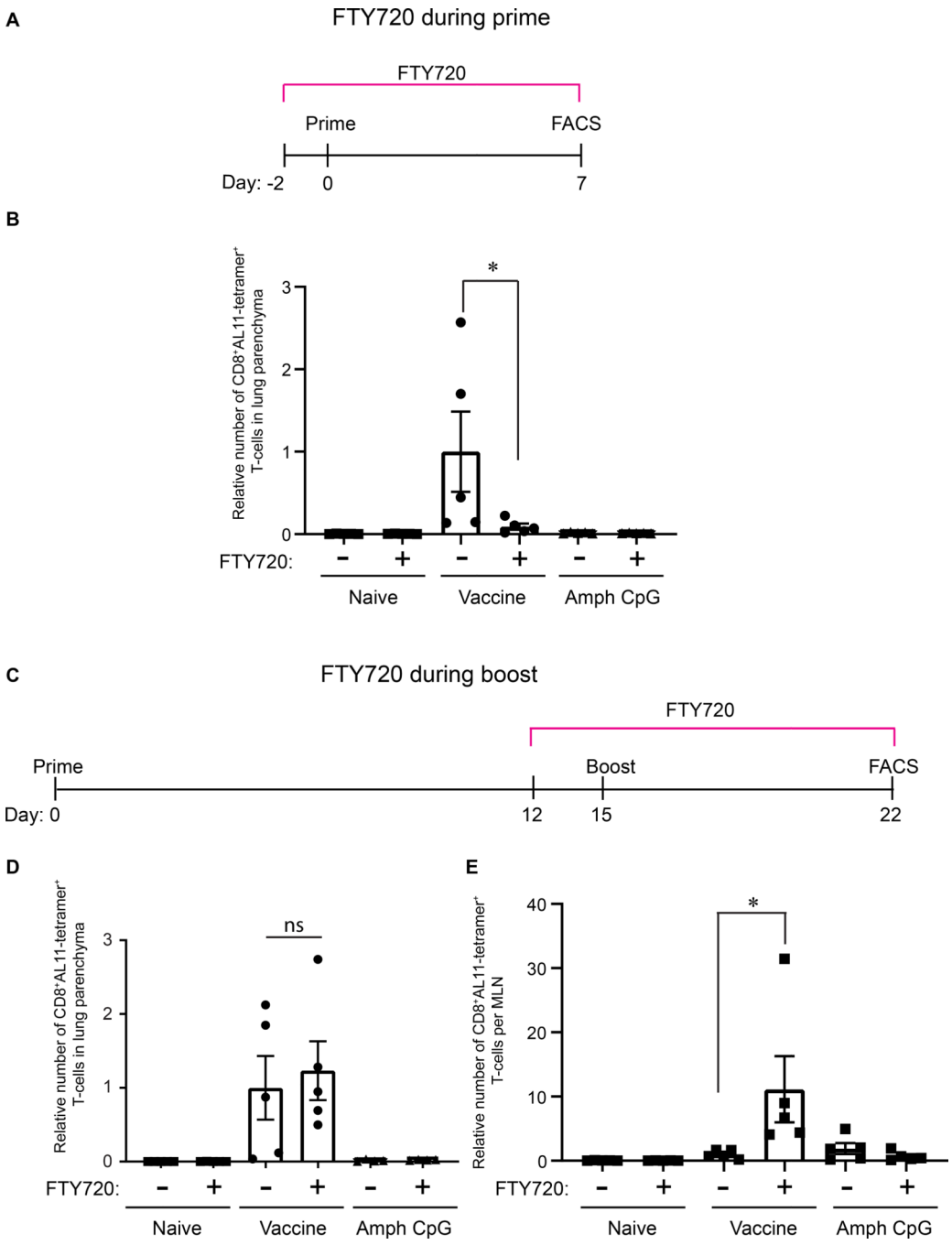

Figure 5: Amph-conjugates elicit T-cell activation directly in lung tissue at boost.

C57BL/6 mice were immunized with amph-conjugated AL11 peptide and CpG in the presence or absence of FTY720 treatment. **(A, C)** Schedule of amph-vaccine delivery in the presence of FTY720 during prime (A) and boost (C) immunizations. **(B)** Quantification of $CD8^+AL11\text{-}tetramer^+$ T cells in the lung parenchyma post prime. **(D, E)** Quantification of $CD8^+AL11\text{-}tetramer^+$ T cells in lungs (D) and MLN (E) 6 days post boost in the presence or absence of FTY720. Data are represented as mean ± SEM, *$p<0.05$, as determined by one-way ANOVA, data are representative of two independent experiments (n = 5 animals/group).

Author Manuscript Author Manuscript Author Manuscript Author Manuscript

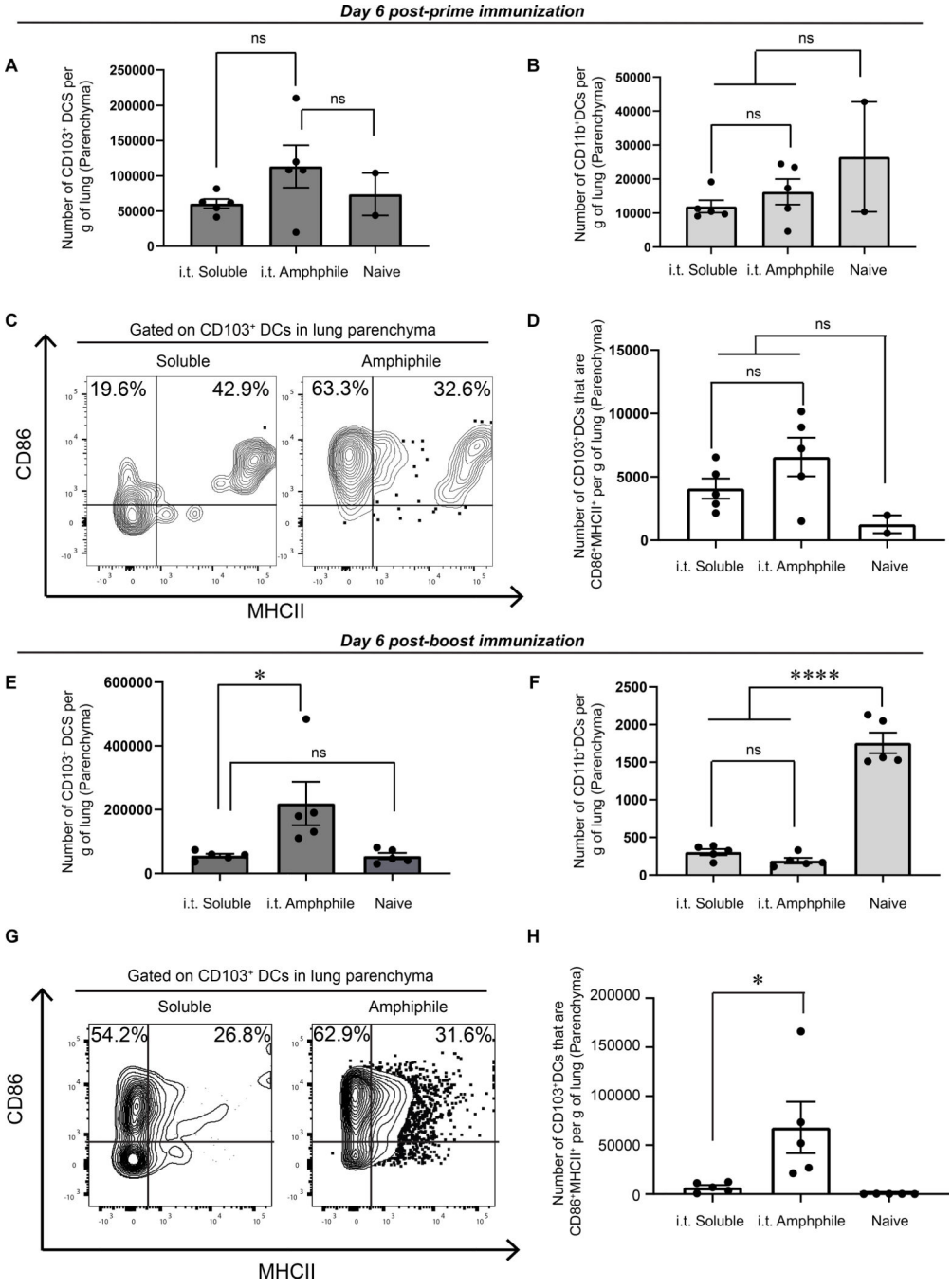

Figure 6: Activated CD103$^+$ DCs are expanded in the lung tissue following booster immunization with amph-vaccines.

C57BL/6 mice were vaccinated on day 0 with 5 μg AL11 and 8 μg CpG or equimolar doses of amph-AL11 and amph-CpG. Tissues were harvested 6 days post prime immunization. **(A, B)** Enumeration of CD103$^+$ (A) and CD11b$^+$ (B) DCs in the lung. **(C)** Representative flow cytometry plots of CD86 and MHC-II expression on lung CD103$^+$ DCs. **(D)** Quantification of lung MHC-II$^+$CD86$^+$CD103$^+$DCs. **(E-H)** C57BL/6 mice were vaccinated on days 0 and 14 with 10 μg gp100 and 8 μg CpG or equimolar doses of amph-gp100 and amph-CpG.

Author Manuscript Author Manuscript Author Manuscript Author Manuscript

Tissues were harvested 6 days post boost immunization. **(E, F)** Quantification of lung $CD103^+$ (E) and $CD11b^+$ (F) DCs. **(G)** Representative flow cytometry plots of CD86 and MHC-II expression on lung $CD103^+$ DCs. **(H)** Quantification of lung MHC-II $^+CD86^+CD103^+$DCs. Data are represented as mean ± SEM, *p<0.05, ****p<0.0001, ns: not significant, as determined by one-way ANOVA; data are representative of at least 2 independent experiments (n = 5 animals/ group).